arXiv:1512.06530v1 [cond-mat.str-el] 21 Dec 2015

Kondo effect in CeX_c (X_c=S, Se, Te) studied by electrical resistivity under high pressure

Yuya Hayashi[1], Shun Takai[1], Takeshi Matsumura[1,2], Hiroshi Tanida[1], Masafumi Sera[1,2], Kazuyuki Matsubayashi[3], Yoshiya Uwatoko[3], and Akira Ochiai[4]

[1]*Department of Quantum Matter, AdSM, Hiroshima University, Higashi-Hiroshima, Hiroshima 739-8530, Japan*

[2]*Institute for Advanced Materials Research, Hiroshima University, Higashi-Hiroshima, Hiroshima 739-8530, Japan*

[3]*Institute for Solid State Physics, University of Tokyo, Kashiwa, Chiba, 277-8581, Japan*

[4]*Department of Physics, Graduate School of Science, Tohoku University, Sendai 980-8578, Japan*

We have measured the electrical resistivity of cerium monochalcogenices, CeS, CeSe, and CeTe, under high pressures up to 8 GPa. Pressure dependences of the antiferromagnetic ordering temperature T_N, crystal field splitting, and the $\ln T$ anomaly of the Kondo effect have been studied to cover the whole region from the magnetic ordering regime at low pressure to the Fermi liquid regime at high pressure. T_N initially increases with increasing pressure, and starts to decrease at high pressure as expected from the Doniach's diagram. Simultaneously, the $\ln T$ behavior in the resistivity is enhanced, indicating the enhancement of the Kondo effect by pressure. It is also characteristic in CeX_c that the crystal field splitting rapidly decreases at a common rate of -12.2 K/GPa. This leads to the increase in the degeneracy of the f state and further enhancement of the Kondo effect. It is shown that the pressure dependent degeneracy of the f state is a key factor to understand the pressure dependence of T_N, Kondo effect, magnetoresistance, and the peak structure in the temperature dependence of resistivity.

1. Introduction

Through the hybridization between conduction electrons and localized f state (c-f hybridization), the f electrons at different atomic sites interact with each other, leading to a magnetic ordered state. This is the Ruderman-Kittel-Kasuya-Yosida (RKKY) interaction. At the same time, the c-f hybridization causes the local spin and orbital degrees of freedom to be screened by the conduction electrons, leading to the reduction of the local moment and the magnetic ordering temperature. This is the Kondo effect. The strength of the c-f hybridization, J_{cf}, is the primary parameter to describe these competing phenomena. In Ce based compounds with one $4f$ electron, the RKKY interaction dominates the Kondo effect when J_{cf} is small, and the magnetic ordering temperature increases with increasing J_{cf}. With further increasing J_{cf}, the Kondo effect gradually dominates the RKKY interaction, and the magnetic ordering temperature starts to decrease. Finally, the magnetic ordering vanishes, and the c-f hybridized system forms a Fermi liquid ground state with heavy effective mass. This general scheme has been described by Doniach's diagram.[1,2] Of particular interest in recent years is in the vicinity of J_{cf} where the magnetic ordering vanishes, which is called the quantum critical point (QCP). In this region, the order parameter fluctuation causes the physical properties to deviate from the Fermi liquid behavior, and in some cases causes unconventional superconductivity.[3–5] In the course of this study, application of pressure is an suitable method to experimentally realize the variation of J_{cf}.

CeS, CeSe, and CeTe, crystallizing in a cubic NaCl-type structure, exhibit antiferromagnetic (AFM) orderings with $\boldsymbol{q} = (\frac{1}{2}, \frac{1}{2}, \frac{1}{2})$ at T_N=8.4, 5.4, and 1.9 K, respectively.[6–8] In a cubic crystalline electric field (CEF), the Hund's rule ground multiplet of $J = 5/2$ splits into the Γ_7 doublet and the Γ_8 quartet. It is already well established that the ground state of CeX_c is the Γ_7 and the energy level of the Γ_8 state is at 140 K, 116 K, and 32 K for CeS, CeSe, and CeTe, respectively.[9–11] The magnitude of the ordered moment in the AFM phase is 0.57 μ_B, 0.56 μ_B, and 0.3 μ_B for CeS, CeSe, and CeTe, respectively. The reduction of the ordered moment from the expected value of 0.71 μ_B for the Γ_7 ground state can be ascribed to the Kondo effect. However, the largest reduction in CeTe cannot be understood from the Kondo effect only, because the Kondo effect is the weakest in CeTe and the strongest in CeS as judged from the $\ln T$ anomaly ($d\rho/d\ln T$) in resistivity.[8] This is still an open question.

In most of the Ce based compounds that have been studied to date under high pressure in the quantum critical region, the CEF ground states are well isolated Kramers doublets, where only the magnetic dipolar de-

gree of freedom plays a role. It is also the case in CeX_c at ambient pressure with the Γ_7 ground state. However, it has been strongly suggested by recent experiments on CeTe that the Γ_8 excited level falls down under high pressure.[12,13] The CEF splitting is expected to vanish at around 2.5 GPa in CeTe. This means that the quadrupolar degree of freedom of the Γ_8 state also takes part in the physical properties at low temperatures. It has already been shown for CeTe that an antiferroquadrupolar interaction through the Γ_8 excited level is essential to understand the properties under high pressure.[13] Therefore, nontrivial phenomenon could take place in the quantum critical region by an interplay between nondipolar degrees of freedom and the Kondo effect. This is also an important issue in relation to the recent studies in Pr based compounds, where the role of quadrupolar fluctuation for the superconductivity attracts interest.[14] High pressure study on CeX_c, therefore, has its significance in studying the possibility of multipolar degrees of freedom to participate in the quantum critical phenomenon.

Another advantage in studying CeX_c lies in its simple electronic structure. The localized f state hybridizes with the p-orbital of X_c, which forms the valence band. The conduction band is formed by the $5d$-orbital of Ce, containing one conduction electron per formula unit. The f level is located ~ 2.3 eV below the Fermi level. These features common in CeX_c have been clarified in detail by the angle-resolved photoemission spectroscopy and the de Haas-van Alphen effect measurements.[15–17]

In the present work, we have measured the electrical resistivity of CeX_c under high pressures up to 8 GPa to study the enhancement of the Kondo effect and the crossover from the magnetic ordering regime to the Fermi liquid regime. We show that the $\ln T$ behavior in the resistivity is enhanced by applying pressure in all the CeX_c compounds. The pressure dependences of T_N, CEF splitting, coefficient of the $\ln T$ term, and the temperatures of resistivity maximum below which the Fermi liquid state is formed, are extracted from the data. Although the overall feature can be understood in the framework of Doniach's diagram, we suggest that the level lowering of the Γ_8 excited state at high pressures gives rise to some distinct phenomena in CeX_c in the crossover region around the QCP. We compare these results with those of other inter-metallic compounds.

2. Experiment

The single crystalline samples were prepared by Bridgman method as described in Ref. 16. Resistivity under high pressure was measured by normal four terminal method. The current direction was along the [001] axis. For measurements up to 2.5 GPa, we used a CuBe/NiCrAl hybrid-piston-cylinder cell with daphne oil as a pressure transmitting medium. Magnetic field was also applied using a 15 T cryomagnet. The field direction was along the [001] axis, which was parallel to the current direction. The measurements up to 8 GPa were performed at zero field using a cubic anvil cell with fluorinert as a pressure transmitting medium.

3. Experimental Results

3.1 Resistivity at zero field

3.1.1 CeTe

Figure 1 (a) shows the temperature (T) dependences of the resistivity (ρ) of CeTe at several pressures. The $\rho(T)$ of LaTe is also shown for reference to estimate the contribution from phonon scattering. At ambient pressure, a hump anomaly is observed around 20 K, reflecting the CEF splitting; ρ decreases below $\sim$ 20 K because the magnetic scattering through the Γ_8 exited state gradually vanishes. We name this characteristic temperature T^*. With further decreasing temperature, ρ drops steeply at 2 K, reflecting the AFM order. The $\ln T$ behavior in $\rho(T)$ due to the Kondo effect can be recognized above T^* after subtracting the $\rho(T)$ of LaTe, whereas it is not recognizable below T^*. These behaviors are consistent with the previous study.[8]

With increasing P, $\rho(T)$ exhibits a clear $\ln T$ dependence below $\sim$ 100 K even before subtracting the $\rho(T)$ of LaTe. This shows that the Kondo effect (single site Kondo scattering) is enhanced by the pressure. If we subtract the $\rho(T)$ of LaTe, the $\ln T$ dependence continues up to 300 K. The hump anomaly at T^* shifts to lower temperatures, corresponding to the level lowering of the Γ_8 exited state.[12] However, above 2.5 GPa, the hump anomaly is no more distinguishable from the peak emerging around 6 K, probably reflecting the Kondo coherence. We name this temperature of resistivity maximum as T_{m1} hereafter. When P is increased from 3.5 GPa to 5 GPa, the coherence peak slightly shifts to higher temperature, which seems to reflect the increase in the Kondo temperature T_K. However, the peak strangely shifts again to lower temperature at 7.3 GPa, which is opposite to the normal P dependence of the coherence peak in Ce based compounds. Although this could be somehow related with the transition to the CsCl structure at 8 GPa in CeTe,[18] the reason is unclear.

The low temperature part of $\rho(T)$ around T_N is shown in the inset of Fig. 2 (a). As indicated by the arrows, T_N of CeTe initially increases with increasing P, and then starts to decrease above $\sim$ 2 GPa. At 3.5 GPa, the anomaly in $\rho(T)$ corresponding to T_N is no more able to be identified. The P dependence of T_N is plotted in Fig. 2 (a). T_N determined from the specific heat measurement in Ref. 13 is also plotted. With respect to the successive transitions at 1.2 GPa and 1.8 GPa reported in Ref. 13, the higher transition temperature agree with T_N deduced from $\rho(T)$. Anomaly corresponding to the second transition at a lower temperature, which is indicated by the filled triangles in Fig. 2 (a), was not detected in $\rho(T)$ as

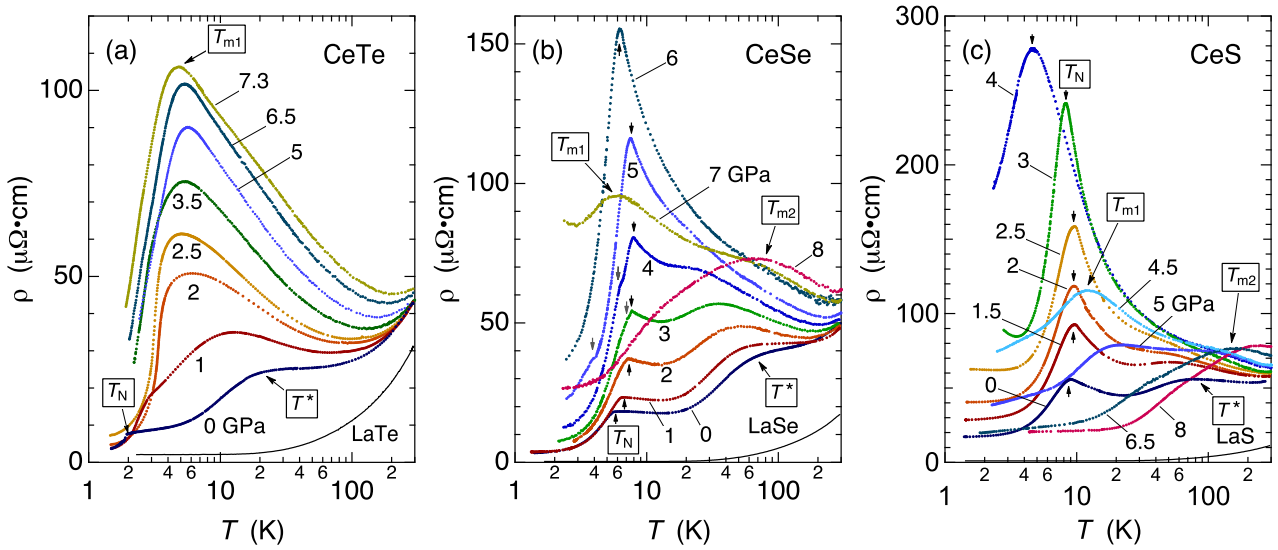

Fig. 1. (Color online) Temperature dependences of the electrical resistivity of (a) CeTe, (b) CeSe, and (c) CeS, under high pressures. The resistivity of LaTe, LaSe, and LaS, at ambient pressure, are also shown for reference.

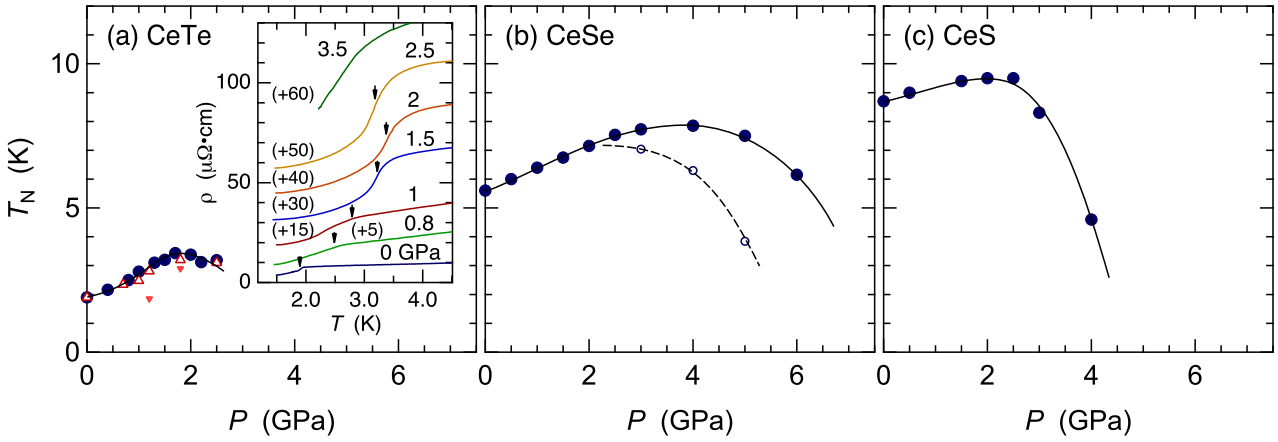

Fig. 2. (Color online) Pressure dependences of T_N of (a) CeTe, (b) CeSe, and (c) CeS, determined from $\rho(T)$ (open circles). The inset of (a) shows $\rho(T)$ of CeTe in the vicinity of T_N. Open and filled triangles in (a) represent the transition temperatures of CeTe determined from the specific heat measurement in Ref. 13. The filled triangles at 1.2 GPa and 1.8 GPa show the successive transitions. Open circles in (b) correspond to the weak anomalies observed in $\rho(T)$ of CeSe below T_N.

a clear anomaly. The critical pressure, P_c, is estimated to be from 3 to 3.5 GPa, although this requires a further study at lower temperatures.

3.1.2 CeSe

Figure 1 (b) shows the $\rho(T)$ curves of CeSe up to 8 GPa. The $\rho(T)$ of LaSe is also shown for reference to estimate the contribution from phonon scattering. At ambient pressure, in the same way as in CeTe, the hump anomaly reflecting the CEF splitting appears at around $T^* = 60$ K and the kink anomaly due to the AFM order is clearly observed at 5.4 K. The $\rho(T)$ weakly increases with decreasing T below $\sim$ 20 K down to T_N. This increase can be ascribed to the Kondo effect within the Γ_7 ground state. The $\ln T$ behavior in the high-T region above T^* can be recognized after subtracting the $\rho(T)$ of LaSe. These behaviors at ambient pressure are consistent with the previous study.[8]

With increasing P, $\rho(T)$ increases and exhibits a clear $\ln T$ anomaly below $\sim$ 200 K, which shows that the Kondo effect (single site Kondo scattering) is enhanced by the pressure. If we subtract the $\rho(T)$ of LaSe, the $\ln T$ dependence continues up to 300 K. Simultaneously, the hump anomaly around T^* shifts to lower tempera-

tures, indicating that the energy level of the Γ_8 exited state falls down with increasing P. Above 5 GPa, T^* is no more recognizable because it is hidden behind the significant increase of $\rho(T)$ due to the Kondo effect.

The $\ln T$ slope below $\sim$ 20 K down to $T_{\rm N}$, where the Kondo effect within the Γ_7 ground state dominates, also increases with P. Above 5 GPa, it is more enhanced and $\rho(T)$ exhibits a steep increase down to $T_{\rm N}$, where a sharp cusp is observed. These behaviors are in contrast to CeTe at high pressures, where $\rho(T)$ follows a single $\ln T$ slope down to $T_{\rm m1} \sim 6$ K and the cusp anomaly at $T_{\rm N}$ soon becomes unclear at high pressures above 2 GPa.

In CeSe, as indicated by the arrows in Fig. 1 (b), $T_{\rm N}$ initially increases with P, taking a maximum at $\sim$ 4 GPa, and decreases. The P dependence of $T_{\rm N}$ is plotted in Fig. 2 (b). The critical pressure, $P_{\rm c}$, is estimated to be around 7.5 GPa. Above 3 GPa, we can also see another weak anomaly in $\rho(T)$ below the main cusp anomaly at $T_{\rm N}$, which is plotted by the open circles. We speculate that this transition reflects some change in the magnetic structure such as the one we discussed in CeTe by a mean-field calculation.[13] Namely, in the intermediate phase, the AFM moment is possibly oriented along the [100] axis because of the Γ_8 level lowering, and in the low-T phase, the direction changes to the [111] axis, reflecting the easy axis of the Γ_7 ground state.

All these behaviors change significantly above 7 GPa, where $\rho(T)$ at low temperatures decreases significantly. At 7 GPa, a new broad peak appears at around 6 K, which we suggest the peak of $T_{\rm m1}$, the same kind of Kondo coherence peak as the one observed in CeTe. The upturn in $\rho(T)$ below 3 K probably suggests the AFM ordering existing below the lowest temperature of 2.5 K. It is also remarked that there is a broad hump anomaly at around 60 K, which we name $T_{\rm m2}$. At 8 GPa, the position of this peak shifts to around 70 K, above which the $\ln T$ behavior is still observed. At low temperatures below 70 K, $\rho(T)$ shows a more significant decrease down to the lowest temperature, suggesting the formation of a Fermi liquid state. Therefore, the broad peak at $T_{\rm m2}$, 60 K at 7 GPa and 70 K at 8 GPa, may also be assigned to another Kondo coherence peak. The coherence peak at $T_{\rm m1}$ still seems to exist at around 15 K, where a broad hump is observed. Thus, the double peak structure in $\rho(T)$ is the characteristic of CeSe in the Fermi liquid regime, and both $T_{\rm m1}$ and $T_{\rm m2}$ shift to higher temperatures with increasing P.

3.1.3 CeS

Figure 1 (c) shows the $\rho(T)$ curves of CeS at high pressures. At ambient pressure, in the same way as in CeTe and CeSe, the hump anomaly reflecting the CEF splitting appears at around $T^* = 70$ K and the cusp anomaly due to the AFM order is clearly observed at 8.7 K. An increase in $\rho(T)$ with decreasing T is observed below $\sim$ 20 K down to $T_{\rm N}$, which can be ascribed to the Kondo effect within the Γ_7 ground state. The slope of the $\ln T$ dependence in the low-T region is larger than that of CeSe. The $\ln T$ dependence is also visible in the high-T region above T^* even before subtracting the $\rho(T)$ of LaS. The largest slopes of the $\ln T$ dependences in CeS at ambient pressure, both in the high- and low-T regions, show that the c-f hybridization is the strongest among the three compounds of CeX_c. These behaviors at ambient pressure are consistent with the previous study.[8]

With increasing P, the $\ln T$ slope increases as in CeTe and CeSe, reflecting the enhancement of the Kondo effect (single site Kondo scattering). A drastic phenomenon in CeS is that $\rho(T)$ in the low-T region increases more steeply than the $\ln T$ slope in the high-T region. This behavior becomes more significant above 2.5 GPa. The increase in $\rho(T)$ on approaching $T_{\rm N}$, which can probably be ascribed to the enhancement of the Kondo effect, is much larger than that of CeSe. With respect to $T_{\rm N}$, it initially increases with increasing P, followed by a maximum around 2 GPa, and decreases to 4.5 K at 4 GPa. The upturn in $\rho(T)$ of 3 GPa below 3.5 K probably suggests another AFM ordering existing below the lowest temperature of 2.8 K. The P dependence of $T_{\rm N}$ is plotted in Fig. 2 (c). The critical pressure, $P_{\rm c}$, is estimated to be around 4.5 GPa.

Above 4.5 GPa, a significant change takes place at low temperatures. Although the $\ln T$ behavior remains at high temperatures above 100 K, $\rho(T)$ at low temperatures decreases significantly with increasing P. At 4.5 GPa, a new broad peak appears at around 12 K, which we suggest the peak of $T_{\rm m1}$, the same kind of Kondo coherence peak as the one observed in CeTe and in CeSe. It is again remarked that there is another broad hump anomaly at around 100 K, which we name $T_{\rm m2}$. With further increasing P, both of these broad peaks shift to higher temperatures. Finally at 8 GPa, the $\rho(T)$ curve becomes like that of a typical Fermi liquid system. However, the two broad peaks at $T_{\rm m1}$ and $T_{\rm m2}$ still remain in $\rho(T)$ at 8 GPa; one is at around 60 K and the other is at around 200 K, both of which may be ascribed to the coherence peak in the same way as in CeSe.

3.2 Magnetoresistance

Figure 3 shows the temperature dependences of electrical resistivity in magnetic fields and under high pressures for CeTe, CeSe, and CeS. All the compounds generally exhibit negative magnetoresistance (MR). In CeTe, the MR effect increases significantly with increasing P. At 1.5 GPa and 2.5 GPa, where the Kondo effect is clearly recognized in the $\ln T$ behavior in $\rho(T)$ at zero field, the ρ value decreases and the peak in $\rho(T)$ at $T_{\rm m1}$, 7 K and 5 K, respectively, shifts to higher temperatures with increasing the field. This is a characteristic behavior observed in concentrated Kondo systems.[19,20] In CeSe and

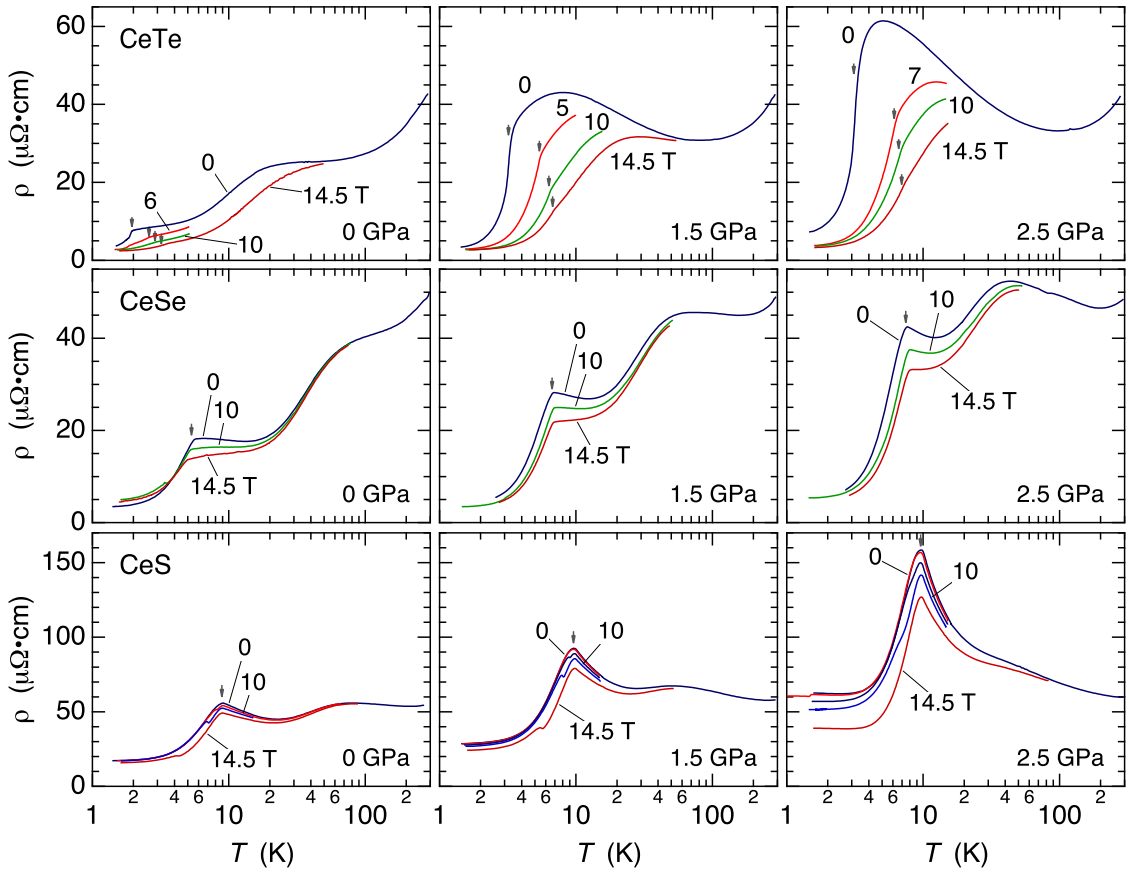

Fig. 3. (Color online) Temperature dependences of electrical resistivity in magnetic fields and under high pressures for CeTe, CeSe, and CeS. Arrows indicate the temperatures of antiferromagnetic ordering.

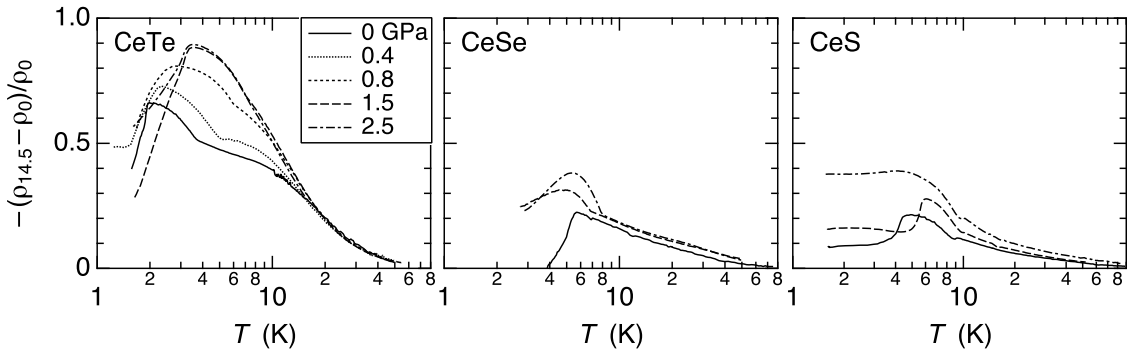

Fig. 4. (Color online) Temperature dependences of the magnetoresistance at 14.5 T, $-(\rho_{14.5} - \rho_0)/\rho_0$, at several pressures.

CeS, by contrast, although the MR effect increases with increasing P, it is not so significant in comparison with that of CeTe. This is because the system is still well inside the magnetic ordering regime at these pressures below 2.5 GPa. The Kondo temperature T_K for the Γ_7 ground state may be much smaller than T_N. In CeTe, on the other hand, T_K is expected to be already larger than T_N at pressures of 1.5 GPa and 2.5 GPa because of the high degeneracy of the ground state due to the almost collapsed CEF.[21,22]

To describe the MR associated with the Kondo effect in more detail, we show in Fig. 4 the temperature dependences of the relative MR at 14.5 T for several pressures. We focus on the temperature range well above T_N: $T > 5$

K for CeTe and $T > 10$ K for CeSe and CeS. The magnitudes of MR in CeSe and CeS are almost the same. If we observe in detail, however, MR is almost independent of P below 2.5 GPa in CeSe, whereas in CeS MR increases slightly with increasing P.

It is noted that CeTe has the largest MR among the three compounds in spite of the fact that J_{cf} is the smallest. This may be because the f-state degeneracy influenced by the low-lying Γ_8 excited level, which increases $T_{\rm K}$, is the largest among the three compounds even at ambient pressure. With increasing P, the MR in CeTe increases below ~ 15 K, and it becomes almost independent of P above 1.5 GPa. It is also remarked that the MR does not change with P above ~ 15 K.

Finally, we comment on the magnetic ordering. In CeTe, $T_{\rm N}$ exhibit a significant dependence both on the applied field and pressure, which can be explained by considering the magnetic and quadrupolar interaction in addition to the Γ_8 level lowering as we have shown in the previous study.[12,13] In CeSe and CeS, by contrast, $T_{\rm N}$ is little affected by the field in this P range below 2.5 GPa. This is because the energy scale of the magnetic interaction is larger than that of CeTe, resulting in larger $T_{\rm N}$, and also because the Γ_8 level is still located at high energy and therefore the level mixing does not affect the magnetic ordering. Finally, although this is not a subject of this work, weak anomalies observed in CeS below $T_{\rm N}$ in Fig. 3, which are clearly identified at 0 GPa and 1.5 GPa in magnetic fields, are those reflecting the change in the magnetic structure or the domain distribution.[10] We can see this phase boundary also in CeSe at 3.5 K in the data at 0 GPa and 10 T. This anomaly moves to $H < 10$ T at 1.5 GPa and 2.5 GPa, which are not shown in Fig. 3.

4. Discussion

In Ce compounds, the coefficient of the $\ln T$ term in the magnetic part of the resistivity, $d\rho_{\rm mag}/d\ln T \equiv S$, is generally associated with $J_{cf}D(\varepsilon_F)$, where $D(\varepsilon_F)$ represents the density of states of the conduction electrons at the Fermi energy. When the system is in the magnetic ordering regime in the Doniach's diagram, as in the present case of CeX_c, the coefficient S and the ρ value at low temperatures generally increase with increasing P. In addition, in this regime, a double peak structure is observed in $\rho_{\rm mag}(T)$ in many systems. The examples are $CeAl_2$, $CeCu_2$, $CeAu_2Si_2$, $CeNiGe_3$, $Ce_2Pd_3Si_5$, and $Ce_2Ni_3Ge_5$.[5,23–28] The peak at high temperature is generally interpreted as reflecting the CEF level splitting of the f state and the second peak at low temperature as the formation of a coherent Kondo state. When the system is near the boundary between the magnetic ordering regime and the Fermi liquid regime, the $\rho_{\rm mag}(T)$ generally exhibit a single peak at around the Kondo coherence temperature, and the peak shifts to high temperatures with increasing P without changing the peak height. The peak position can finally reach to 300 K. The peak of CEF seems to be merged with the coherence peak. The examples are $CeIn_3$, $CeAl_3$ and $CeCu_6$.[4,29–31] To discuss the pressure dependence of these characteristic temperatures of CeX_c, in Fig. 5 we plot $T_{\rm N}$, T^*, $T_{\rm m1}$, $T_{\rm m2}$, and the slope S, which have been deduced from $\rho_{\rm mag}(T)$, as a function of pressure. $\rho_{\rm mag}(T)$ was obtained by subtracting $\rho(T)$ of LaX_c. We discuss these parameters in the following. The most important and distinctive feature we consider in CeX_c is the shrinking of the CEF under pressure, which is reflected in the P dependence of T^*. This effect leads to the increase in the f-state degeneracy and, therefore, the increase in $T_{\rm K}$.[21,22]

First, we discuss the P dependence of the $\ln T$ term in $\rho(T)$. When the CEF anomaly around T^* is at high enough temperatures, we can extract two different coefficients of the $\ln T$ term from high-T and low-T regions above and below T^*, which we represent as $S_{\rm H}$ and $S_{\rm L}$, respectively. Pressure dependences of these coefficients are also shown in the bottom panels of Fig 5. In CeTe, since T^* is soon merged into a peak at $T_{\rm m1}$, only $S_{\rm H}$ is shown. In CeSe and CeS, the two regions are clearly separated up to the critical pressure $P_{\rm c}$ where $T_{\rm N}$ vanishes. With respect to the pressure dependence of $S_{\rm H}$, they almost coincide with each other at high pressures, although $S_{\rm H}$ of CeS is slightly larger than others at $P = 0$. We also see that the increasing rate of $S_{\rm H}$ with pressure is almost the same in CeX_c. On the other hand, $S_{\rm L}$ for CeS is almost ten times larger than that of CeSe and $S_{\rm L}$ for CeTe is unable to recognize, which is probably because the Kondo scattering in CeTe is too small and is hidden behind the magnetic scattering due to disordered moments. This difference in $S_{\rm L}$ shows that the Kondo effect in the low-T region within the Γ_7 ground state is the strongest in CeS and the weakest in CeTe. By contrast, the similar values of $S_{\rm H}$ seems to suggest that the Kondo effect in the high-T region is more influenced by the f-state degeneracy involving all the CEF states than the c-f hybridization effect.

Another point to be noted is that $S_{\rm L}$ exceeds $S_{\rm H}$ in CeSe and in CeS at high pressures. Theoretically, the $\ln T$ coefficient is associated with the degeneracy, λ, of the f state and is proportional to $\lambda^2 - 1$.[32] In the high-T region, $\lambda = 6$, and in the low-T region when only the Γ_7 ground state is thermally populated, $\lambda = 2$. Therefore, $S_{\rm H}$ is generally larger than $S_{\rm L}$, which is actually the case in many other inter-metallic compounds.[5,23] In this sense, CeSe at low pressures is normal. Although the larger increasing rate of $dS_{\rm L}/dP$ than $dS_{\rm H}/dP$ is also observed in $CeAl_2$,[23] it is particularly anomalous in CeSe and CeS that $S_{\rm L}$ exceeds $S_{\rm H}$.

Next, with respect to $T_{\rm N}$, T^*, $T_{\rm m1}$, and $T_{\rm m2}$, a general behavior observed in other inter-metallic compounds in the magnetic ordering regime can be summarized as the

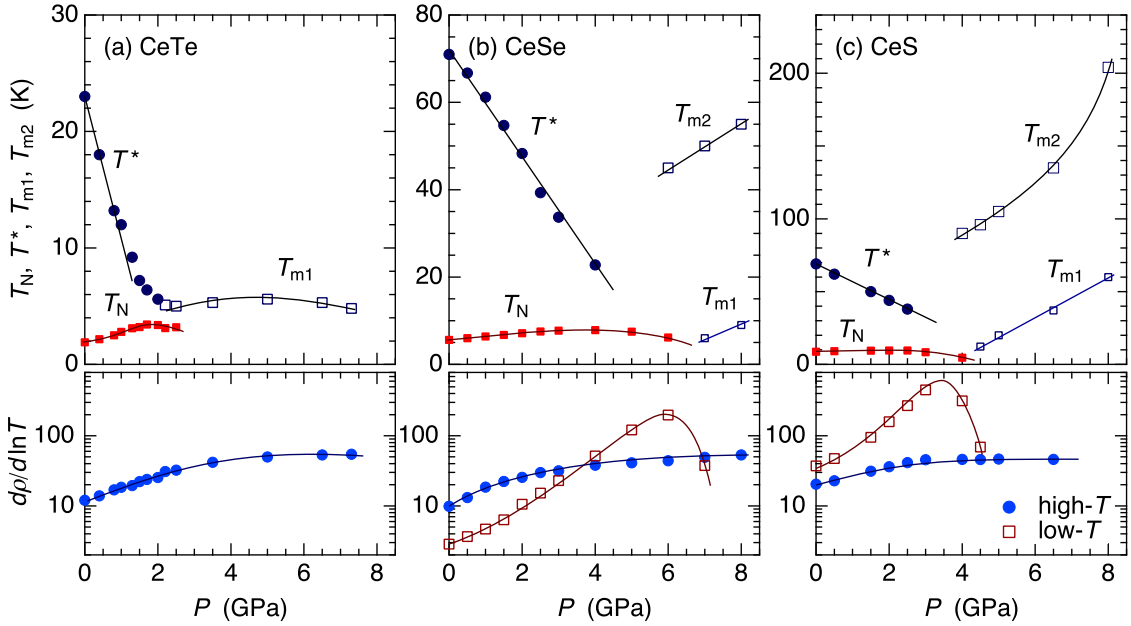

Fig. 5. (Color online) (Top panels) Pressure dependences of the characteristic temperatures T_N, T^*, T_{m1}, and T_{m2}. The lines are guides for the eye. It is remarked that all the three lines for T^* are expressed as $T^*(P) = T^*(0) - 12.2P$. (Bottom panels) Pressure dependences of the coefficient of the $\ln T$ term in the magnetic part of the resistivity, $d\rho_{mag}/d\ln T$, which are estimated in the high-T region above T^* or T_{m2} and in the low-T region between T_N and T^* or between T_{m1} and T_{m2}.

following (see Fig. 3 of Ref. 5 or Fig. 2 of Ref. 23):

(1) Double peaks appear at T^* and T_{m1} ($T^* > T_{m1}$). With increasing P, T^* slightly decreases and T_{m1} slightly increases.

(2) Around P_c, T_{m1} starts to increase rapidly and marge with T^*. Then, a single peak remains in $\rho(T)$ and T^* is renamed to T_{m2}, below which the Fermi liquid state is formed.

(3) T_{m2} increases with increasing P.

These behaviors are actually reproduced by a theory including the CEF effect.[33] However, the behavior of these characteristic temperatures in CeX_c is slightly different:

(1) T^* decreases with increasing P much more rapidly at a rate of -12.2 K/GPa.

(2) T^* and T_{m2} seems not to be connected in CeSe and in CeS. Double peak structure is still observed above P_c.

The slight decrease of T^* with P in general cases means that the true CEF level does not actually change with P. In the present cases of CeX_c, however, the rapid decrease of T^* with P seems to show that the actual CEF splitting decreases with P.[12,13] This is the most important and distinctive feature we consider in CeX_c, which is associated with the f-state degeneracy and the increase in T_K. This effect might also be associated with the anomalous increase of S_L at high pressures.

The critical pressure P_c could also be affected by the pressure dependent CEF splitting. From Fig. 2 we see that P_c is the largest in CeSe and the lowest in CeTe. Although the P dependence of T_N of CeX_c each follows that of the Doniach's diagram, this sequence of P_c does not coincide with the that of the strength of J_{cf}, which is the smallest in CeTe and the largest in CeS. Here, it is necessary to take into account the difference in the CEF splitting, i.e., the largest in CeS and the smallest in CeTe. Especially in CeTe, the CEF splitting soon vanishes at around 2 GPa, where T_N starts to decrease. The smallest P_c in CeTe can be understood by considering the increased degeneracy of the f state due to the collapsed CEF, which results in the increase of T_K than that of CeSe and CeS. Then, T_N of CeTe vanishes at the smallest pressure among the three compounds.

We consider that the pressure dependence of T_N in Fig. 2 can be understood as a result of three effects. Firstly, with increasing P, J_{cf} increases, which results in the increase in the RKKY interaction and T_N. Secondly, the Γ_8 CEF level falls down, which also contributes to the increase in T_N because the Γ_8 state can give rise to larger magnetic moment. This is explained in Ref. 13 for CeTe by using a mean-field model calculation. These two effects both contribute to the increase in T_N. Thirdly, T_K increases with P through the increase of both J_{cf} and the f-state degeneracy. In the present case of CeX_c, we sug-

gest that the latter effect influences T_K more than J_{cf}.

The MR effect can also be roughly explained. In CeSe and CeS below 2.5 GPa, the Γ_8 state is still well separated and the MR effect reflects the suppression of the Kondo effect within the Γ_7 ground state by the applied field. To understand the weak MR effects in CeSe and CeS shown in Fig. 4, Fig. 2 of Ref. 20 based on a periodic Anderson model is a good reference. With increasing P, T_K of the Γ_7 ground state increases, and the scaled parameters of T/T_K and H/T_K decrease. Since we are in the region of $T/T_K > 1$, the increase of MR by the decrease of T/T_K would be cancelled by the decrease of H/T_K. Then, the MR effect is expected to be weak in CeSe and CeS. To analyze in more detail to understand the larger P dependence of MR in CeS than in CeSe, it is necessary to consider that J_{cf} is larger in CeS than in CeSe (see S_L in Fig. 5) and also that the pressure region of $0 \sim 2.5$ GPa in CeS is more close to P_c, or the pressure where S_L takes the maximum. It is also necessary to take into account the gradual increase of f state degeneracy at high pressures.

The much larger MR effect in CeTe should be more related to the higher degeneracy due to the small CEF splitting, which almost vanishes above 1.5 GPa. Although J_{cf} in CeTe is the smallest among the three compounds, the larger degeneracy of the f-state enhances the Kondo effect and leads to the large MR effect. It is remarked that, in Fig. 4, MR of CeTe increases with P up to 1.5 GPa and becomes almost independent of P above 1.5 GPa. This coincides with the shrinking process of CEF which is demonstrated by the variation of T^* in Fig. 5(a). Above 1.5 GPa, the degeneracy of the ground state do not increase any more with P, and then the MR effect changes little with P, which may be understood in the same way as in CeSe and in CeS by the decrease of T/T_K and H/T_K. Above 15 K, where the Γ_8 excited level is well populated, the f state can be recognized as being fully degenerate, and the MR shows little P dependence.

Finally, although we have studied a wide region of pressure, temperature, and magnetic field space, we remark that there still remain a low temperature region below 2 K that should be studied in future. As shown by the $\rho(T)$ curves in Fig. 1, the ρ values at 2 K are still much higher than the residual resistivities, which are expected from the extrapolation of the $\rho(T)$ curves at 0 GPa. This shows that the system has not yet fallen to the ground state, especially near pressures around P_c, and there remain a possibility that some drastic phenomena occur below 2 K.

5. Conclusion

We have studied the Kondo effect in CeS, CeSe, and CeTe by the electrical resistivity measurements under high pressures up to 8 GPa. The $\ln T$ term in the temperature dependence of the resistivity commonly increases with increasing pressure, indicating that the c-f hybridization increases with pressure. There are two $\ln T$ regions. One is at high temperatures, where both Γ_7 and Γ_8 states are involved, and the other is at low temperatures, where the Γ_7 ground state is mainly involved, resulting in the peak structure in $\rho(T)$ around T^* reflecting the CEF splitting. From the $\ln T$ term in the low temperature region, we see that J_{cf} is the largest in CeS and the smallest in CeTe.

CeX_c under high pressure starts from the magnetic ordering regime and the pressure dependence of T_N can basically be understood from the Doniach's diagram. However, it is necessary to take into account the significant decrease and collapse of the CEF splitting under pressure to interpret the sequence of the critical pressure, where T_N vanishes; $P_c(\mathrm{CeTe}) < P_c(\mathrm{CeS}) < P_c(\mathrm{CeSe})$, which contradicts with the sequence of J_{cf}. We suggest that the increase in T_K under high pressure, which is brought about more by the increase of the f-state degeneracy than by the increase of J_{cf}, is responsible for the pressure dependence of T_N and magnetoresistance.

Finally, the appearance of the double peak structure in $\rho(T)$ in CeSe and CeS at high pressures near and above P_c is also a distinctive feature in CeX_c. Since T^* seems to be connected to the low-temperature peak at T_{m1}, the second peak at T_{m2} may suggest an appearance of another energy scale associated with the formation of the Kondo singlet state. In any case, however, this is an open question to be studied in future.

Acknowledgements

This work was carried out by the joint research in the Institute for Solid State Physics, the University of Tokyo, and was supported by JSPS KAKENHI Grant Numbers 2430087 and 15K05175.

1) S. Doniach, Physica B+C **91**, 231 (1977).
2) J. Otsuki, H. Kusunose, and Y. Kuramoto, J. Phys. Soc. Jpn. **78**, 034719 (2009).
3) H. v. Löhneysen, A. Rosch, M. Vojta, and P. Wölfle, Rev. Mod. Phys. **79**, 1015 (2007).
4) G. Knebel, D. Braithwaite, P. C. Canfield, G. Lapertot, and J. Flouquet, Phys. Rev. B **65**, 024425 (2001).
5) Z. Ren, L. V. Pourovskii, G. Giriat, G. Lapertot, A. Georges, and D. Jaccard, Phys. Rev. X **4**, 031055 (2014).
6) F. Hulliger, B. Natterer, and H. R. Ott, J. Magn. Magn. Mater. **8**, 87 (1978).
7) H. R. Ott, J. K. Kjems, and F. Hulliger, Phys. Rev. Lett. **42**, 1378 (1979).
8) J. Schoenes and F. Hulliger, J. Magn. Magn. Mater. **63&64**, 43 (1987).
9) J. Rossat-Mignod, J. M. Effantin, P. Burlet, T. Chattopadhyay, L. P. Regnault, H. Bartholin, C. Vettier, O. Vogt, D. Ravot, and J. C. Achart, J. Magn. Magn. Mater. **52**, 111 (1985).
10) A. Dönni, A. Furrer, P. Fisher, S. M. Hayden, F. Hulliger, and T. Suzuki, J. Phys: Condens. Matter **5**, 1119 (1993).
11) A. Dönni, A. Furrer, P. Fisher, and F. Hulliger, Physica B

186-188, 541 (1993).
12) Y. Kawarasaki, T. Matsumura, M. Sera, and A. Ochiai, J. Phys. Soc. Jpn. **80**, 023713 (2011).
13) H. Takaguchi, Y. Hayashi, T. Matsumura, K. Umeo, M. Sera, and A. Ochiai, J. Phys. Soc. Jpn. **84**, 044708 (2015).
14) K. Matsubayashi, T. Tanaka, A. Sakai, S. Nakatsuji, Y. Kubo, and Y. Uwatoko, Phys. Rev. Lett. **109**, 187004 (2012).
15) M. Nakayama, H. Aoki, A. Ochiai, T. Ito, H. Kumigashira, T. Takahashi, and H. Harima, Phys. Rev. B **69**, 155116 (2004).
16) M. Nakayama, N. Kimura, H. Aoki, A. Ochiai, C. Terakura, T. Terashima, and S. Uji, Phys. Rev. B **70**, 054421 (2004).
17) G. Chiaia, L. Duò, O. Tjernberg, M. Göthelid, M. Björkqvist, H. Kumigashira, S.-H. Yang, T. Takahashi, T. Suzuki, and I. Lindau, Phys. Rev. B **57**, 12030 (1998).
18) J. M. Leger, R. Epain, J. Loriers, D. Ravot, and J. Rossat-Mignod, Phys. Rev. B **28**, 7125 (1983).
19) A. Takase, K. Kojima, T. Komatsubara, and T. Kasuya, Solid State Commun. **36**, 461 (1980).
20) N. Kawakami and A. Okiji, J. Phys. Soc. Jpn. **55**, 2114 (1986).
21) K. Yamada, K. Yosida, and K. Hanzawa, Prog. Theor. Phys. **71**, 450 (1984).
22) K. Hanzawa, K. Yamada, and K. Yosida, J. Magn. Magn. Mater. **47&48**, 357 (1985).
23) H. Miyagawa, G. Oomi, M. Ohashi, I. Satoh, T. Komatsubara, M. Hedo, and Y. Uwatoko, Phys. Rev. B **78**, 064403 (2008).
24) E. Vargoz, P. Link, D. Jaccard, T. Le Bihan, and S. Heathman, Physica B **229**, 225 (1997).
25) P. Link and D. Jaccard, Physica B **230**, 31 (1997).
26) M. Nakashima, K. Tabata, A. Thamizhavel, T. C. Kobayashi, M. Hedo, Y. Uwatoko, K. Shimizu, R. Settai, and Y. Ōnuki, J. Phys: Condens. Matter **16**, L255 (2004).
27) N. Kurita, H. Yamamoto, M. Hedo, T. Fujiwara, T. Shigeoka, S. W. Tozer, and Y. Uwatoko, Physica B **403**, 1479 (2008).
28) M. Nakashima, H. Kohara, A. Thamizhavel, T. D. Matsuda, Y. Haga, M. Hedo, Y. Uwatoko, R. Settai, and Y. Ōnuki, J. Phys: Condens. Matter **17**, 4539 (2005).
29) T. Kagayama, T. Ishii, and G. Oomi, J. Alloys and Compounds **207-208**, 263 (1994).
30) G. Oomi and T. Kagayama, J. Phys. Soc. Jpn. **65**, 2732 (1996).
31) S. Raymond and D. Jaccard, Journal of Low Temperature Physics **120**, 107 (2000).
32) B. Cornut and B. Coqblin, Phys. Rev. B **5**, 4541 (1972).
33) Y. Nishida, A. Tsuruta, and K. Miyake, J. Phys. Soc. Jpn. **75**, 064706 (2006).